



Improvement of cell response of the poly(lactic-co-glycolic acid)/calcium phosphate cement composite scaffold with unidirectional pore structure by the surface immobilization of collagen via plasma treatment

Fupo He^a, Jiyan Li^a, Jiandong Ye^{a,b,*}

^a School of Materials Science and Engineering, South China University of Technology, Guangzhou 510641, China

^b National Engineering Research Center for Tissue Restoration and Reconstruction, Guangzhou 510006, China

ARTICLE INFO

Article history:

Received 27 July 2012

Received in revised form 1 October 2012

Accepted 9 October 2012

Available online 17 October 2012

Keywords:

Calcium phosphate cement

PLGA

Collagen

Scaffold

Cell response

Plasma treatment

Unidirectional lamellar pore

ABSTRACT

In this study, calcium phosphate cement (CPC)-based scaffold with unidirectional lamellar pore structure was fabricated by unidirectional freeze casting. Poly(lactic-co-glycolic acid) (PLGA) was infiltrated into the CPC scaffold to improve its strength and toughness, which compromised the bioactivity and osteoconductivity of CPC. Collagen (Col) was immobilized on the pore surface of the PLGA/CPC scaffold to enhance the bioactivity of the scaffold using plasma treatment under the ammonia (NH₃) atmosphere. The immobilization of collagen was characterized by infrared spectroscopy (ATR-FTIR), X-ray photoelectron spectroscopy (XPS) and scanning electron microscopy (SEM). Compared to the PLGA/CPC composite scaffold, the Col/PLGA/CPC composite scaffold had higher contact angle, porosity and water absorption, while the compressive strength of both scaffolds was comparable. Rat bone marrow mesenchymal stem cells (rMSCs) seeded on the Col/PLGA/CPC scaffold showed markedly improved cell seeding, attachment, proliferation and differentiation than those on the PLGA/CPC scaffold. These results suggest that the surface immobilization of collagen by plasma treatment can improve the bioactivity of the PLGA/CPC scaffold and the Col/PLGA/CPC composite scaffold is a promising candidate for bone tissue engineering.

© 2012 Elsevier B.V. All rights reserved.

1. Introduction

Calcium phosphate cement (CPC) has been proved to be extremely biocompatible and osteoconductive, which was demonstrated by the fast deposition of new bone on the cement surface [1,2]. Thereby CPC has been widely used as bone tissue engineering scaffold [3,4]. However, like other bioceramic scaffolds, brittleness and low strength are intrinsic drawbacks to be resolved for the CPC scaffold. Coating polymer [(poly(lactic acid), poly(lactic-co-glycolic acid) (PLGA) and polycaprolactone, etc.)] on the scaffold surface is an effective approach to improve the mechanical property of the bioceramic scaffolds [5–8]. PLGA is a FDA-approved material that has been widely used as surgical suture material, drug carrier, and tissue engineering scaffold material due to its good mechanical property, biocompatibility, and adjustable biodegradability [9–11]. Nevertheless, PLGA has poor cell–matrix interaction because of lacking natural recognition sites on its surface [12], and functional groups for further modification [13]. If the CPC scaffold is reinforced by PLGA coating, the polymer coating on the pore wall of CPC scaffold will prevent the bioactive CPC matrix from

contacting directly with tissues/organs, which compromises the biological advantages of CPC. Hence, the surface bioactivity of polymer-coated CPC scaffold needs to be improved.

Plasma treatment is a conventional method to modify the surface property of polymers [14–16]. By the use of plasma treatment, reactive sites such as amino groups and carboxyl can be created on the surfaces of polymers without changing other bulk properties such as mechanical and biodegradable properties. However, the practical application of plasma-treated polymers is limited because of short preserving time [14]. Immobilization of bioactive molecules on the plasma-treated polymer surface was reported as an effective method to address the weakness of short preserving time [17–19]. Collagen, which accounts for 90% of the extracellular matrix of natural bone, is beneficial for cell adhesion and growth and has low immune response [20]. Moreover, the degradation products of collagen are not harmful to tissue and cells [20]. Therefore, collagen is commonly used as a bioactive coating on the polymeric materials [19,21].

Unidirectional freeze-drying is an effective method to fabricate polymer or inorganic scaffolds with unidirectional pore structure, high porosity and pore interconnectivity [22,23]. The unidirectional pores facilitate cells and tissue ingrowth throughout the scaffold [24]. On the basis of our previous studies on the PLGA/CPC composite scaffold with unidirectional lamellar pore structure [25,26],

* Corresponding author. Tel.: +86 20 22236283; fax: +86 20 87111752.

E-mail address: jdye@scut.edu.cn (J. Ye).

herein collagen was immobilized on the surface of the PLGA/CPC scaffold using plasma treatment under the ammonia (NH_3) atmosphere to improve the cell response of the composite scaffold. Physical and chemical properties and in vitro biological properties (cell attachment, proliferation and differentiation) of the Col/PLGA/CPC composite scaffolds were assessed.

2. Materials and methods

2.1. Materials

The CPC powder used in this study was prepared by mixing partially crystallized calcium phosphate (PCCP, median diameter of $16.5\ \mu\text{m}$) with dicalcium phosphate anhydrous (DCPA, median diameter of $3.7\ \mu\text{m}$) at a weight ratio of 1:1, as described in our previous articles [27,28]. PCCP was synthesized from an aqueous solution of $\text{Ca}(\text{NO}_3)_2 \cdot 4\text{H}_2\text{O}$ ($0.36\ \text{mol/L}$) and $(\text{NH}_4)_2\text{HPO}_4 \cdot 12\text{H}_2\text{O}$ ($0.15\ \text{mol/L}$) by chemical precipitation method in our laboratory. The deposits were washed to fully eliminate the remnants of NO_3^- and NH_4^+ , then centrifugally separated, freeze-dried and calcined at 450°C for 2 h in a furnace to partially crystallize. The as-calcined PCCP powders were milled in a planetary mill using ZrO_2 balls at 400 rpm for 2 h. DCPA, glutaraldehyde and glycine were commercially obtained from Shanghai No. 4 Reagent & H. V. Chemical Co. Ltd., China. Sodium alginate as setting accelerator was purchased from Tianjin Fuchen Chemical Reagent Co. Ltd., China. PLGA (75/25 lactide to glycolide ratio, MW: 100,000, the inherent viscosity of $1.39\ \text{dL/g}$) was purchased from Jinan Daigang Biomaterials Co. Ltd., China. Type I collagen was purchased from Shanghai Qisheng Biomaterials Co. Ltd., China. Cell-culture related reagents were purchased from Gibco (Invitrogen, USA) except specialized.

2.2. Preparation of PLGA/CPC scaffold

The method for fabrication of PLGA/CPC scaffold has been described in previous studies [25,26]. The CPC slurry was prepared by mixing the 2 wt% (W/V) sodium alginate solution with the CPC powder at the liquid to CPC powder ratio of 3.25 mL/g. Then the slurry was poured into the cylindrical glass (with an inner diameter of 7 mm and a height of 14 mm) and immediately put on a cold plane to freeze. Temperature difference from bottom (-30°C) to top (room temperature) of slurry caused the orientational crystallization of ice. The frozen samples were freeze-dried for 48 h to obtain the unidirectional macropores. The macroporous CPC samples were incubated in the incubator with 98% relative humidity at 37°C for 7 days to make sure sufficient setting reaction of CPC. PLGA was dissolved in dichloromethane (CH_2Cl_2) at the fraction of 0.20 g/mL (W/V) to form a flowable solution. The porous CPC samples were immersed in the PLGA solution, followed by vacuum infiltration in a vacuum desiccator for 5 h. After infiltration procedure, the samples were air-dried for at least 48 h to eliminate the remained CH_2Cl_2 .

2.3. Immobilization of collagen on the surface of PLGA/CPC scaffold

The plasma treatment of the PLGA/CPC scaffold samples was performed using a Omega Plasma Processor (DL-1, OPS Plasma, China) under the NH_3 atmosphere. PLGA/CPC scaffold samples were first suspended in the plasma chamber. Then the chamber was evacuated until the air pressure decreased to less than 10 Pa by a vacuum pump. The pressure was adjusted to maintain at 20 Pa when NH_3 was vented to the plasma chamber. The electrical power was 50 W and the treatment time was 10 min. The NH_3 plasma-treated PLGA/CPC scaffolds were immersed in 4 mg/mL collagen solution at 4°C and infiltrated under the low vacuum

for 0.5 h, followed by incubation in a collagen solution for 3 h at 4°C . The obtained samples were rinsed with deionized water to remove the excess collagen. The samples were cross-linked with 0.02 wt% glutaraldehyde aqueous solution for 24 h, then immersed in 0.1 M glycine aqueous solution for 2 h to remove the free aldehyde groups. After that, the samples were rinsed with deionized water, then freeze-dried.

2.4. Materials characterization

2.4.1. Morphological characterization

The morphology of the composite scaffolds was observed with an environmental scanning electron microscope (Quanta 200, FEI, the Netherlands). After being dried, the scaffold samples were mounted on an aluminum stub by carbon tape and sputtered with gold. An accelerating voltage of 2–15 kV was used to characterize the morphology of composite scaffolds.

2.4.2. ATR-FTIR spectroscopy and X-ray photoelectron spectroscopy

FTIR spectra were recorded on a Bruker (Germany) Vector 33 IR analyzer equipped with an attenuated total reflectance (ATR) accessory, which provided surface analysis. The spectra consisted of 16 scans and measured at a resolution of $4\ \text{cm}^{-1}$ in the spectral range of $4000\text{--}600\ \text{cm}^{-1}$. The surface elemental composition of the composite scaffolds was analyzed by XPS (Axis Ultra DLD, Kratos, Britain). A standard Al $K\alpha$ excitation source (1.5 kV, 10 mA) was employed.

2.4.3. Static contact angle

As shown in Fig. 1, the pore surface of the PLGA/CPC scaffold was basically fully covered by PLGA film with hardly any CPC matrix exposed. Therefore, the measurements of the surface contact angles of the scaffolds were conducted on the PLGA films. The PLGA solution at the concentration of 0.2 g/mL (W/V) was cast into the polytetrafluoroethylene mold. The PLGA film was obtained after complete vaporization of CH_2Cl_2 . The NH_3 plasma-treated and collagen-immobilized PLGA films were obtained according to the aforementioned methods. Static contact angles of the films were measured with a contact angle analyzer (OCA15, Dataphysics, Germany) using the sessile drop technique at 25°C . The measurements were carried out in the air with water as the probe liquid. The static contact angle was the average of six different sites on the films.

2.4.4. Water absorption

The water absorption of the scaffolds was measured by the following procedure. After being immersed in deionized water at 37°C for 6 h, the scaffolds were taken out, then the water on the surface of the scaffolds was wiped off gently with a wet sponge, followed by immediately measuring the weight of the scaffolds. The water absorption was calculated with the following equation:

$$\text{Water absorption} = \frac{W_1 - W_0}{W_0} \times 100\%$$

where W_0 and W_1 denote the weight of the scaffolds before and after being immersed in water, respectively. The water absorption of the scaffolds was the average of six replicates.

2.4.5. Compressive strength test

The compressive strength of the cylindrical scaffolds (diameter = 7 mm, height = 14 mm) was measured using a universal material testing machine (INSTRON 5567, INSTRON, Britain) at a crosshead speed of 0.5 mm/min. Six replicates were tested for each scaffold and the average value was calculated.

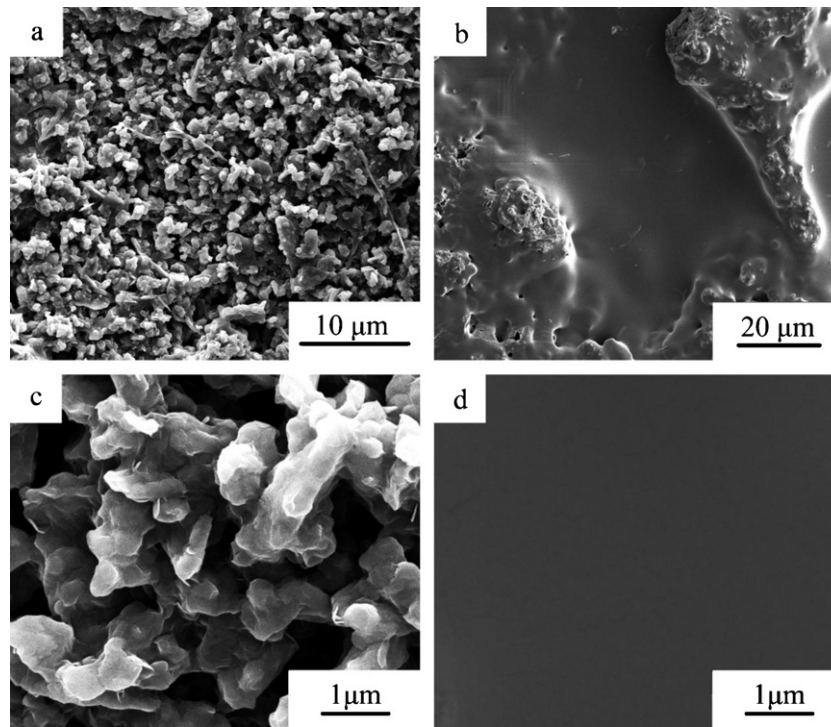


Fig. 1. Surface morphology of the internal pore wall of CPC scaffold (a, c) and PLGA/CPC composite scaffold (b, d).

2.4.6. Porosity determination

The porosity of the scaffolds was measured using a Archimedes technique with ethanol as the displacement liquid. The weight of a dried sample was recorded as G_1 and the weight of a specific gravity bottle full of ethanol as G_2 . The scaffold sample was put into the bottle and evacuated under vacuum for 0.5 h to remove the air in the scaffold sample. The weight of the bottle together with ethanol and scaffold sample was recorded as G_3 . The weight of the scaffold sample full of ethanol was measured as G_4 . The porosity (P) of the composite scaffold was calculated using the following equation:

$$P = \frac{G_4 - G_1}{G_4 - (G_3 - G_2)} \times 100\%$$

The porosity of the scaffolds was the average of six replicates.

2.5. Rat bone marrow mesenchymal stem cells (rMSCs) harvest

rMSCs were obtained from bilateral femora of Fischer 344/N syngeneic rats. Both femora were cut away from the epiphysis of the rat. Bone marrow was flushed out of the marrow cavity with 15 mL of culture medium minimal essential medium eagle (MEME) containing 10% fetal bovine serum (FBS) and 1% antibiotics (100 U/mL penicillin G, 100 μ g/mL streptomycin sulfate and 0.25 μ g/mL amphotericin B). The bone marrow suspension was transferred into a 75 cm² tissue culture polystyrene flask and incubated at 37 °C in a humidified incubator with 5% CO₂. The culture medium was refreshed every 3 days to remove dead cells and wastes produced by metabolism of cells. After about 90% confluence was reached, the rMSCs were passaged.

2.6. Cell culture and cell seeding

The Col/PLGA/CPC scaffolds and PLGA/CPC scaffolds (control) were cut into disks with 7 mm in diameter and 2.5 mm in height. After being sterilized by gamma radiation (15 kGy), the disks were put into 24-well plates and pre-wetted with MEME solution for

12 h. rMSCs at passage 1 were used. For assays of cell attachment and proliferation, 35 μ L of cell suspension (10⁶ cells/mL) was seeded onto the surface of the samples in 24-well plates. The cell-seeded samples were incubated at 37 °C in a humidified incubator with 5% CO₂ for 2 h to allow the cells to adhere onto the sample surface, followed by addition of 1 mL of culture medium to each well to cover the sample. The culture medium was renewed every 3 days.

2.7. Cell attachment and proliferation

The morphology and distribution of rMSCs cultured on the scaffolds were observed using a Live/Dead kit (Biotium, USA) according to standard protocol provided by the manufacturer. Only "Live" assay was performed in this study. The stained cell-sample constructs were observed under a fluorescence microscope (Zeiss Axioskop 40, Germany). In addition, the scaffold constructs were cut along the direction parallel to the pore orientation to observe the penetration of rMSCs into the internal pores.

Cell proliferation was evaluated by WST-8 assay using a CCK-8 kit (Dojindo Laboratories, Japan) according to the manufacturer's instructions.

2.8. Alkaline phosphatase (ALP) activity

40 μ L of cell suspension (2.5 \times 10⁶ cells/mL) was seeded onto each sample in 24-well plate. Then 1 mL of culture medium (MEME supplemented with 10% FBS, 10 mM sodium β -glycerophosphate, 10 nM dexamethasone and 82 mg/mL vitamin C) was added. After being cultured for 7 and 14 days, the cell-sample constructs were washed twice with PBS. An aliquot of 400 μ L of 0.05% Triton X was added into each well, and the mixture was incubated at 4 °C for 2 h. The supernatant was tested for total protein content and ALP activity. Total protein content was assayed by the Bradford method using a Bio-Rad protein assay reagent kit (Bio-Rad Laboratories Inc., Japan) according to the manufacturer's instructions.

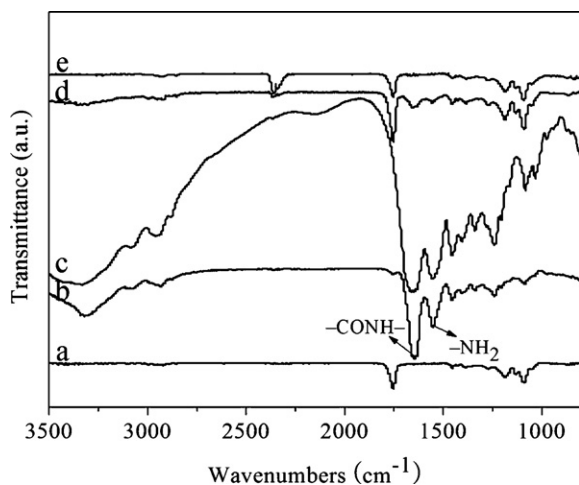


Fig. 2. ATR-FTIR spectra of collagen and various treated PLGA/CPC scaffolds: (a) PLGA/CPC composite scaffold; (b) Col/PLGA/CPC composite scaffold; (c) Pure collagen; (d) Col/PLGA/CPC scaffold after being extensively rinsed with deionized water; (e) collagen-coated PLGA/CPC scaffold without NH_3 plasma treatment after being extensively rinsed with deionized water.

The ALP activity of the rMSCs was assayed using a Laboassay™ ALP kit (Wako Pure Chemicals, Japan) in accordance with the manufacturer's instructions.

2.9. Statistics/data analysis

All data points are an average of at least three replicates and expressed as mean \pm standard deviation (SD). Statistical comparisons were performed by one-way analysis of variance (ANOVA) for multiple comparisons. A value of $p < 0.05$ was considered statistically significant.

3. Results

3.1. ATR-FTIR

FTIR spectra of the PLGA/CPC scaffold surface before and after various treatments are shown in Fig. 2. Both the ester bond at $1000\text{--}1300\text{ cm}^{-1}$ and carbonyl peak ($\text{C}=\text{O}$ stretching) at 1737 cm^{-1} appeared on all the scaffold surfaces, while no characteristic peak of PO_4^{3-} appeared. After collagen was immobilized on the surface of PLGA/CPC scaffold, two new strong vibration peaks appeared at 1650 and 1550 cm^{-1} , which corresponded to amide I ($-\text{CONH}-$) and amide II ($-\text{NH}_2$) (Fig. 2b). The peak shape of the FTIR spectrum of Col/PLGA/CPC scaffold surface was similar to that of pure collagen (Fig. 2c). After being extensively rinsed with deionized water, those obvious vibration peaks at 1650 and 1550 cm^{-1} were still present (Fig. 2d). As for PLGA/CPC scaffold coated with collagen layer without plasma treatment, the peaks at 1650 and 1550 cm^{-1} disappeared after being extensively washed (Fig. 2e), and the resulting FTIR spectrum was similar to that of PLGA/CPC scaffold without any treatment (Fig. 2a).

3.2. XPS

The elemental composition of the surface of the PLGA/CPC scaffold before and after modification was identified by XPS analysis (Fig. 3a). Calcium (Ca) and phosphorus (P) were detected on the surfaces of all scaffolds. The XPS quantitative analysis of the PLGA/CPC scaffold surface exhibited that Ca and P only comprised 3.65% and

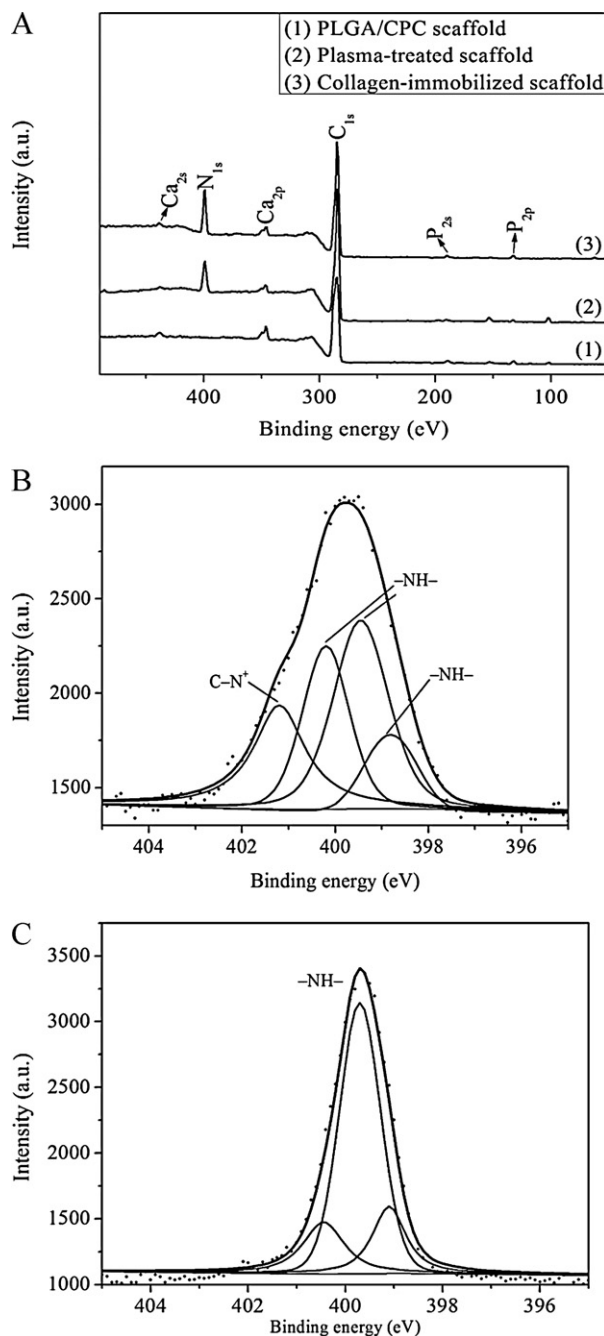


Fig. 3. XPS survey scan spectra of surfaces of PLGA/CPC scaffold, NH_3 plasma-treated PLGA/CPC scaffold and Col/PLGA/CPC scaffold (a). Deconvoluted N_{1s} spectra of NH_3 plasma-treated PLGA/CPC scaffold (b) and Col/PLGA/CPC scaffold (c).

2.15% of the surface compositions of the PLGA/CPC scaffold, respectively. XPS spectra of plasma-treated and collagen-immobilized PLGA/CPC scaffolds exhibited a new peak at 400.0 eV , which corresponded to the nitrogen element (N_{1s}). The deconvoluted N_{1s} spectra of the plasma-treated scaffold and collagen-immobilized scaffold are shown in Fig. 3b and c. The original N_{1s} spectrum of the plasma-treated scaffold was resolved into four components with binding energies of 398.8 , 399.5 , 400.2 and 401.2 eV , of which the former three binding energies were attributed to $-\text{NH}-$ while the last one to polaron $-\text{C}-\text{N}^+$. The deconvoluted N_{1s} spectrum of the collagen-immobilized scaffold was assigned to $-\text{NH}-$ (399.1 , 399.7 and 400.5 eV).

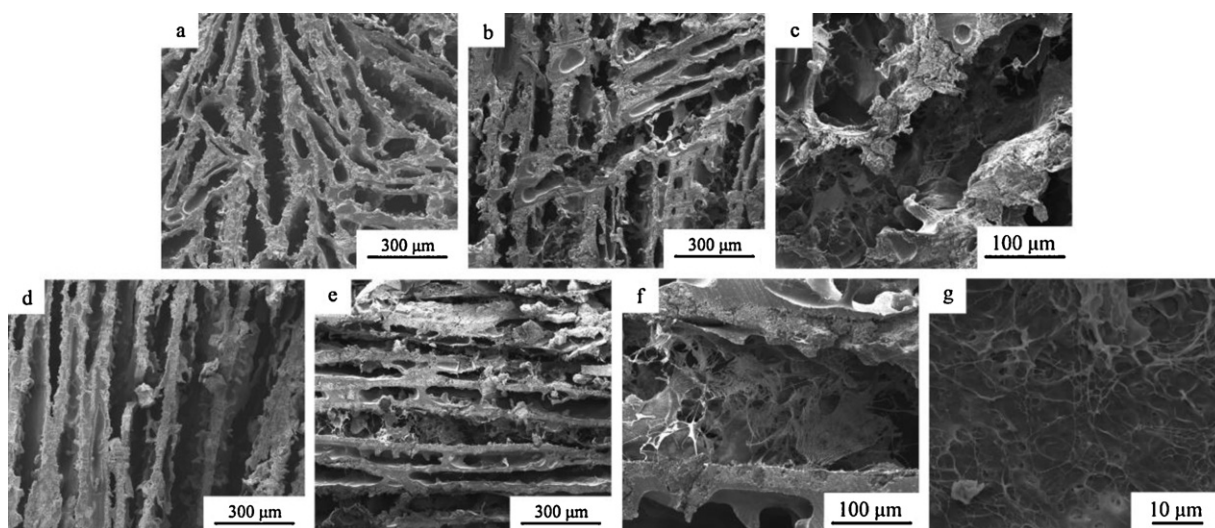


Fig. 4. SEM micrographs of PLGA/CPC scaffold (a, d) and Col/PLGA/CPC scaffold (b, c, e–g) under different magnifications. Parts (a–c) represent the cross section perpendicular to the long axis of the cylindrical sample. Parts (d–f) represent the cross section parallel to the long axis of the cylindrical sample, and (g) represents the surface morphology of the internal pore wall of Col/PLGA/CPC scaffold.

3.3. SEM

The morphology of the PLGA/CPC scaffold before and after immobilization of collagen is shown in Fig. 4. The PLGA/CPC scaffold sample showed unidirectional lamellar pores with width in the range of 100 μm –150 μm , and length larger than 300 μm even up to 1–2 mm (Fig. 4a and d). After immobilization of collagen, the pore surface was covered by the collagen layer (Fig. 4g), and the internal macropores of the scaffold were filled with reticular collagen fibers. The scaffold still maintained high interconnectivity with the existence of collagen.

3.4. Contact angle, water absorption, porosity and compressive strength

The contact angle of the PLGA film before and after surface modification is shown in Fig. 5a. The contact angle on the PLGA film was $76.6 \pm 2.8^\circ$, and decreased to $25.3 \pm 1.1^\circ$ after being treated by NH_3 plasma. When collagen was immobilized on the surface of PLGA film, the contact angle sharply increased to $103.7 \pm 3.8^\circ$. The water absorption, porosity and compressive strength of the PLGA/CPC scaffold before and after modification are shown in Fig. 5b–d. The water absorption of the PLGA/CPC scaffold was $36.63 \pm 3.95\%$. After being treated by NH_3 plasma, it increased to $58.94 \pm 3.70\%$. Furthermore, after collagen was immobilized on the surface of the PLGA/CPC scaffold, the water absorption reached $67.49 \pm 5.50\%$, which was nearly two times as high as that of PLGA/CPC scaffold without modification (Fig. 5b).

The porosity of the PLGA/CPC scaffold was $58.50 \pm 2.50\%$. After NH_3 plasma treatment and further immobilization of collagen, the porosity of the scaffold increased to $63.50 \pm 3.39\%$ and $63.84 \pm 1.30\%$, respectively (Fig. 5c). The compressive strength of the PLGA/CPC scaffold was 5.04 ± 0.44 MPa, after plasma treatment and further immobilization of collagen, the compressive strength of the scaffold was 5.19 ± 0.21 MPa and 5.16 ± 0.52 MPa, respectively (Fig. 5c).

3.5. Cell attachment

The morphology and distribution of rMSCs cultured on the PLGA/CPC scaffold and Col/PLGA/CPC scaffold were evaluated after 1, 3 and 7 days of culture (Fig. 6). Compared to the PLGA/CPC

scaffold, the Col/PLGA/CPC scaffold exhibited much more cells with better spread and elongated shape. After 7 days of culture, the cells nearly fully covered the outer surface of the Col/PLGA/CPC scaffold. With respect to PLGA/CPC scaffold, unremarkable cell proliferation was observed on its outer surface compared to that on the 3rd day. No cell was visible in the internal pores of both scaffolds on the 3rd day. After 7 days of culture, the cells migrated into the internal pores of both scaffolds.

3.6. Cell proliferation

The cell proliferation on the Col/PLGA/CPC scaffold and PLGA/CPC scaffold is shown in Fig. 7a. After 1 day of culture, the cell number on the Col/PLGA/CPC scaffold was higher than that on the PLGA/CPC scaffold. As culture time prolonged, the cell number on both the scaffolds increased, and the difference in cell number on the Col/PLGA/CPC scaffold and PLGA/CPC scaffold also increased. Fig. 7b shows the cell growth rate on the PLGA/CPC scaffold and Col/PLGA/CPC scaffold. On the 3rd day, the cell growth rate on the Col/PLGA/CPC scaffold was slightly higher than that on the PLGA/CPC scaffold ($65.16 \pm 12.22\%$ versus $63.10 \pm 24.85\%$). Nevertheless, after 7 days of culture, the cell growth rate on the Col/PLGA/CPC scaffold was significantly higher than that on the PLGA/CPC scaffold ($132.84 \pm 41.25\%$ versus $46.83 \pm 20.63\%$).

3.7. ALP activity

The ALP activity of rMSCs on the PLGA/CPC scaffold and Col/PLGA/CPC scaffold on the 7th and 14th day is shown in Fig. 8. On day 7, the ALP activity of rMSCs on the PLGA/CPC scaffold was much lower than that on the Col/PLGA/CPC scaffold. After 14 days of culture, ALP activity of rMSCs on both the scaffolds increased, while the cells on the Col/PLGA/CPC scaffold exhibited a significantly higher ALP activity than those on the PLGA/CPC scaffold.

4. Discussion

In our previous studies, a PLGA/CPC scaffold with unidirectional lamellar pore structure was fabricated [25,26]. SEM images of the pore surface of PLGA/CPC scaffold showed that PLGA film covered the surface of the CPC matrix (Fig. 1), which indicated that bioactive CPC matrix was prevented from interacting with cells and tissue by

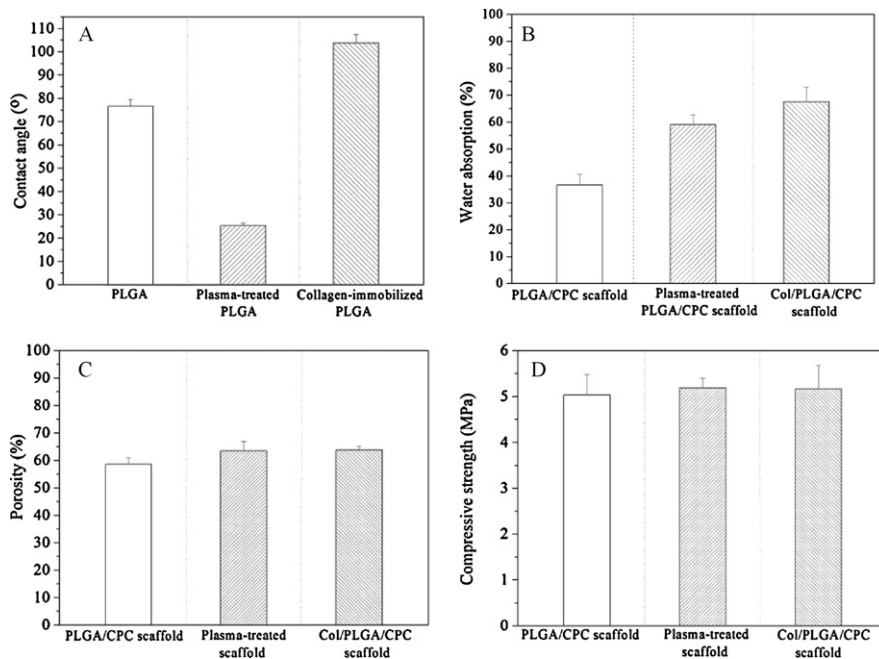


Fig. 5. Contact angle (a), water absorption (b), porosity (c) and compressive strength (d) of PLGA/CPC scaffold, NH_3 plasma-treated PLGA/CPC scaffold and Col/PLGA/CPC scaffold. Data presented as mean \pm SD, $n=6$.

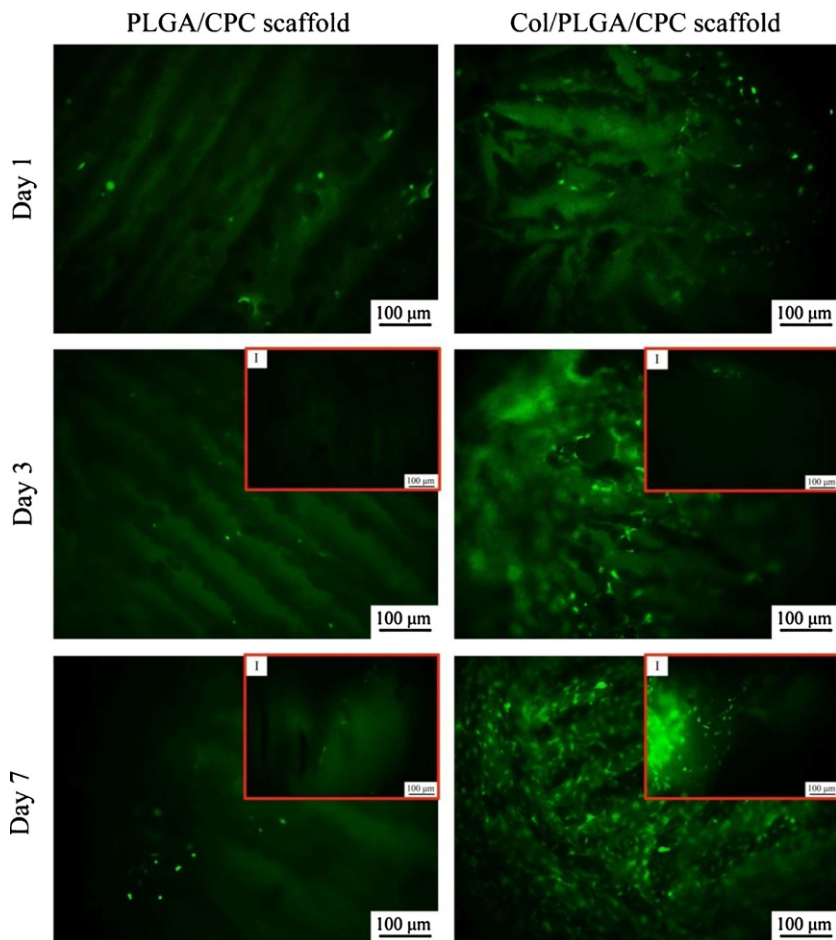


Fig. 6. Fluorescence photographs of rMSCs on the PLGA/CPC scaffold and Col/PLGA/CPC scaffold after 1, 3 and 7 days of culture. (I) represents the photograph of the interior of PLGA/CPC scaffold or Col/PLGA/CPC scaffold after 3 or 7 days of culture.

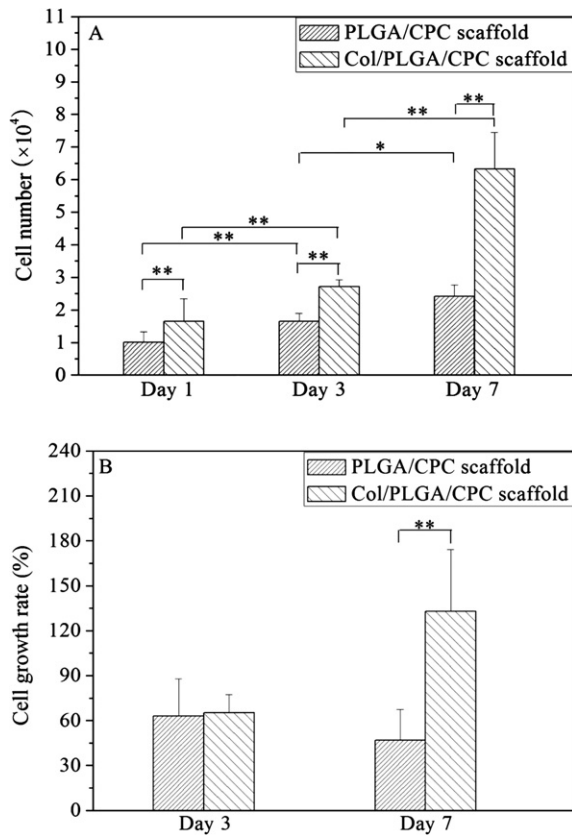


Fig. 7. Proliferation of rMSCs on the PLGA/CPC scaffold and Col/PLGA/CPC scaffold (a). Cell growth rate on the PLGA/CPC scaffold and Col/PLGA/CPC scaffold on the 3rd (against the 1st day) and the 7th (against the 3th day) day (b). Data presented as mean \pm SD, $n=3$. * $p < 0.05$, ** $p < 0.01$.

PLGA film. Therefore, it is necessary to improve the cell response of the composite scaffold. SEM images, XPS spectrum and FTIR spectrum of the pore surface of PLGA/CPC scaffold demonstrated that the surface components of PLGA/CPC scaffold were dominated by PLGA (Figs. 1–3). In this case, the surface modification of PLGA/CPC scaffold was mainly focused on the PLGA film. Coating collagen is a common method to improve surface wettability and cell response of synthetic polymer scaffold. However, physically adsorbed collagen coating on the polymer surface is liable to be removed from the scaffold surface. By using the plasma treatment, abundant polar groups, which can bond to biomolecules by polar interaction and hydrogen bonding, are introduced onto the surface of polymeric material [29]. In this study, we immobilized the collagen on the

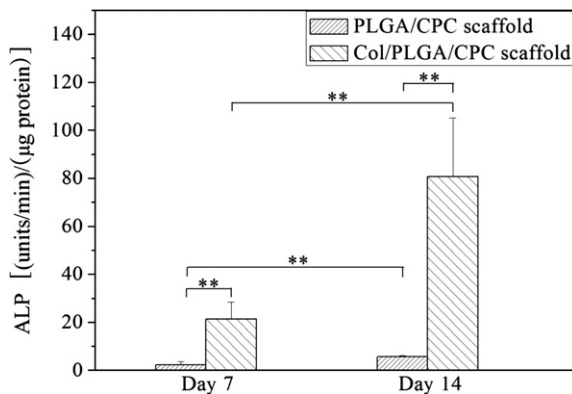


Fig. 8. ALP activity of rMSCs on the PLGA/CPC scaffold and Col/PLGA/CPC scaffold after 7 and 14 days of culture. Data presented as mean \pm SD, $n=3$. * $p < 0.05$, ** $p < 0.01$.

surface of PLGA/CPC scaffold by the plasma treatment under the NH_3 atmosphere.

As shown in Fig. 3b, $-\text{NH}-$ and $-\text{C}-\text{N}^+$ were deposited on the surface of PLGA/CPC scaffold after the NH_3 plasma treatment. The pK_a values of $-\text{NH}-$ and collagen are 10.5 and 4.8, respectively. Hence, at pH 7.2, $-\text{NH}-$ and collagen display positive and negative charges, respectively. In this case, collagen can be immobilized on the surface of NH_3 plasma-treated PLGA/CPC scaffold by polar interaction, hydrogen bonding and electrostatic interactions between these opposite charges, as reported by Yang and Bei [29] and Feng et al. [30]. Enriched $-\text{NH}-$, which were detected on the surface of Col/PLGA/CPC scaffold, originated from the amino acid sequence of the collagen molecules. FTIR spectra exhibited that the spectral shape of Col/PLGA/CPC scaffold was similar to that of pure collagen irrespective of peak intensity (Fig. 2b and c). This indicates that the PLGA/CPC scaffold was covered by collagen layer, which was supported by the SEM observation of the Col/PLGA/CPC scaffold surface (Fig. 4g). After being extensively washed with deionized water, the two characteristic vibration peaks for $-\text{NH}_2$ and $-\text{CONH}-$ were still visible (Fig. 2d). As for collagen-coated PLGA/CPC scaffold without NH_3 plasma treatment, the characteristic peaks disappeared (Fig. 2e). The results of ATR-FTIR analysis demonstrated that the binding force between collagen and PLGA/CPC scaffold was enhanced by pretreatment of NH_3 plasma, which made the collagen immobilized on the scaffold surface. SEM images of the Col/PLGA/CPC scaffold showed that besides covering the pore surface of the scaffold, collagen also partly filled in the macropores of the scaffold with reticular formation. Nevertheless, the Col/PLGA/CPC scaffold retained unidirectional lamellar macroporous structure and high pore interconnection, providing space for the ingrowth of cells and new bone tissue (Fig. 4).

Compared to PLGA film, the contact angle of the NH_3 plasma-treated PLGA film decreased significantly due to the introduced hydrophilic groups ($-\text{NH}-$ and $\text{C}-\text{N}^+$). However, the contact angle of the collagen-immobilized PLGA surface markedly increased. This is because the collagen used in this study had structural integrity, which caused higher contact angle [31]. The high water absorption of scaffold can promote the infiltration of cell solution into the scaffold and facilitate cell seeding [21]. Compared to the PLGA/CPC scaffold, the water absorption of NH_3 plasma-treated PLGA/CPC scaffold markedly increased due to the introduction of hydrophilic groups. The further increase in water absorption of Col/PLGA/CPC scaffold was caused by high water affinity of the collagen. Plasma treatment does not change the bulk properties of materials such as mechanical and biodegradable properties. Consequently, the compressive strength of NH_3 plasma-treated scaffold remained unchanged. Furthermore, the compressive strength of Col/PLGA/CPC scaffold also hardly changed because of extremely low mechanical strength of collagen. The porosity of scaffolds was measured using the Archimedes method with ethanol in this study. $-\text{OH}$ of ethanol is easy to combine with $-\text{NH}-$ by hydrogen bond. In this case, compared to the PLGA/CPC scaffold, more ethanol could be taken by NH_3 plasma-treated PLGA/CPC scaffold and Col/PLGA/CPC scaffold due to rich $-\text{NH}-$ groups on the surface of both scaffolds. Consequently, plasma-treated PLGA/CPC scaffold and Col/PLGA/CPC composite scaffold presented a higher porosity than the PLGA/CPC scaffold, even though collagen occupied a small part of space in the Col/PLGA/CPC scaffold.

rMSCs on the Col/PLGA/CPC scaffold exhibited better spread and elongation than those on the PLGA/CPC scaffold (Fig. 6). As shown in Fig. 7a, on the 1st day, the cell number on the Col/PLGA/CPC scaffold was 1.5 times as high as that on the PLGA/CPC scaffold, which indicated that the cell seeding rate of Col/PLGA/CPC scaffold was much higher than that of PLGA/CPC scaffold. The higher cell

seeding rate of the Col/PLGA/CPC scaffold was attributed to that the collagen layer immobilized on the scaffold provided natural adhesion sites for cell attachment, and the reticular collagen filled in the macropores of the scaffold hindered the cells from falling off the scaffold [28]. As prolongation of culture time, much higher cell growth rate on the Col/PLGA/CPC scaffold than that on the PLGA/CPC scaffold can also be explained by the bioactivity of collagen, whose effect on cell attachment and proliferation has been well confirmed [19–21]. ALP activity is considered as an early stage marker of osteogenic differentiation of rMSCs because it degrades the organic phosphoesters in bone, which promotes the deposition of calcium minerals in bone [32]. In the present study, the ALP activity on the Col/PLGA/CPC scaffold was significantly higher than that on the PLGA/CPC scaffold. Seyedjafari et al. [33] and Salaszyk et al. [34] reported that collagen was beneficial for osteogenic differentiation. Thereby the collagen was contributive to the increase in ALP activity on the Col/PLGA/CPC scaffold. In addition, the fast cell proliferation on the Col/PLGA/CPC scaffold may lead to cell aggregation, which also promoted the cell differentiation [35].

Collagen, PLGA and CPC are commonly used as scaffold materials. However, single material cannot meet requirements of an excellent scaffold. Low mechanical strength and fast degradation inhibit application of plain collagen scaffold [36]. Poor bioactivity and stiffness are the main problems for plain PLGA scaffold to be solved [37]. Brittleness and low mechanical strength are intrinsic defects of plain CPC scaffold [38]. In the present study, the collagen on the surface of Col/PLGA/CPC composite scaffold is beneficial for cell adhesion and proliferation and osteogenic differentiation at the early stage of implantation. PLGA bears a large proportion of the mechanical load applied on the scaffold. Although the mechanical strength of the scaffold decreases with gradual degradation of PLGA film on the surface of the porous CPC matrix when implanted, more and more CPC matrix can be exposed to the surrounding tissue simultaneously, which facilitates new bone regeneration in the composite scaffold. Consequently, the ingrowth of new bone tissue can compensate the decrease in mechanical strength caused by degradation of PLGA. In a word, the Col/PLGA/CPC composite scaffold with unidirectional pore structure can meet the requirements at various stages after implantation *in vivo*.

5. Conclusion

The collagen was immobilized on the surface of PLGA/CPC scaffold by NH_3 plasma treatment to obtain a Col/PLGA/CPC composite scaffold with unidirectional lamellar pore structure, suitable compressive strength and bioactive surface. Compared to the PLGA/CPC scaffold, contact angle, water absorption and porosity of the Col/PLGA/CPC scaffold increased while the compressive strength remained unchanged. The cell seeding, attachment, proliferation and differentiation on the Col/PLGA/CPC composite scaffold were markedly better than those on the PLGA/CPC composite scaffold. The Col/PLGA/CPC composite scaffold fabricated in this study is a promising candidate for eligible bone tissue engineering scaffold due to its satisfactory biocompatibility and cell response.

Acknowledgements

This work was supported by the National Natural Science Foundation of China (NSFC) under Grant No. 51172074 and the National Basic Research Program of China under Grant No. 2012CB619100 as well as the Program for Changjiang Scholars and Innovative Research Team in University under Grant No. IRT0919.

References

- [1] E.M. Ooms, J.G.C. Wolke, J.P.C.M. van der Waerden, J.A. Jansen, *J. Biomed. Mater. Res.* 61 (2002) 9.
- [2] L. Comuzzi, E. Ooms, J.A. Jansen, *Clin. Oral Implants Res.* 13 (2002) 304.
- [3] S. Takagi, L. Chow, *J. Dent. Res.* 74 (SI) (1995) 559.
- [4] T. Yoshikawa, Y. Suwa, H. Ohgushi, S. Tamai, K. Ichijima, *Biomed. Mater. Eng.* 6 (1996) 345.
- [5] J. Chevalier, L. Gremillard, *J. Eur. Ceram. Soc.* 29 (2009) 1245.
- [6] R. Zhang, P.X. Ma, *J. Biomed. Mater. Res.* 44 (1999) 446.
- [7] X. Miao, D.M. Tan, J. Li, R. Crawford, *Acta Biomater.* 4 (2008) 638.
- [8] J. Zhao, L.Y. Guo, X.B. Yang, J. Weng, *Appl. Surf. Sci.* 255 (2008) 2942.
- [9] X. Shi, Y. Wang, R.R. Varshney, L. Ren, Y. Gong, D.A. Wang, *Eur. J. Pharm. Sci.* 39 (2010) 59.
- [10] P.Q. Ruhé, E.L. Hedberg, N.T. Padron, P.H.M. Spauwen, J.A. Jansen, A.G. Mikos, *J. Biomed. Mater. Res. A* 74 (2005) 533.
- [11] B.D. Ulery, L.S. Nair, C.T. Laurencin, *J. Polym. Sci. Polym. Phys.* 49 (2011) 832.
- [12] D.A. Barrera, E. Zylstra, P.T. Lansbury, R. Langer, *J. Am. Chem. Soc.* 115 (1993) 11010.
- [13] R.C. Thomson, M.J. Yaszemski, J.M. Powers, A.G. Mikos, *J. Biomater. Sci. Polym. Ed.* 7 (1996) 23.
- [14] (a) H. Shen, X. Hu, F. Yang, J. Bei, S. Wang, *Biomaterials* 28 (2007) 4219; (b) H. Shen, X. Hu, F. Yang, J. Bei, S. Wang, *Surf. Coat. Technol.* 98 (1998) 1102.
- [15] M. Nakagawa, F. Teraoka, S. Fujimoto, Y. Hamada, H. Kibayashi, J. Takahashi, *J. Biomed. Mater. Res.* 77 (2006) 112.
- [16] C.M. Alves, Y. Yang, J.L. Ong, V.L. Sylvia, D.D. Dean, C.M. Agrawal, R.L. Reis, *Biomaterials* 28 (2007) 307.
- [17] J. Marchand-Brynaert, E. Detrait, O. Noiset, T. Boxus, Y.J. Schneider, C. Remacle, *Biomaterials* 20 (1999) 1773.
- [18] J. Marchand-Brynaert, M. Deldime, I. Dupont, J.L. Dewez, Y.J. Schneider, *J. Colloid Interface Sci.* 173 (1995) 236.
- [19] J. Yang, J.Z. Bei, S.G. Wang, *Biomaterials* 23 (2002) 2607.
- [20] W. Friess, *Eur. J. Pharm. Biopharm.* 45 (1998) 113.
- [21] G. Chen, A. Okamura, K. Sugiyama, M.J. Wozniak, N. Kawazoe, S. Sato, T. Tateishi, *J. Biomed. Mater. Res. B* 90 (2009) 864.
- [22] S.R. Mukai, H. Nishihara, H. Tamon, *Chem. Commun.* (2004) 874.
- [23] H. Zhang, I. Hussain, M. Brust, M.F. Butler, S.P. Rannard, A.I. Cooper, *Nat. Mater.* 4 (2005) 787.
- [24] M.M.C.G. Silva, L.A. Cyster, J.J.A. Barry, X.B. Yang, R.O.C. Oreffo, D.M. Grant, C.A. Scotchford, S.M. Howdle, K.M. Shakesheff, F.R.A.J. Rose, *Biomaterials* 27 (2006) 5909.
- [25] X. Qi, J. Ye, Y. Wang, *J. Biomed. Mater. Res. A* 89 (2009) 980.
- [26] F. He, J. Ye, *J. Biomed. Mater. Res. A* 100 (2012) 3239.
- [27] X. Wang, J. Ye, Y. Wang, X. Wu, B. Bai, *J. Biomed. Mater. Res. A* 81 (2007) 781.
- [28] X. Wang, J. Ye, Y. Wang, *J. Mater. Sci. Mater. Med.* 19 (2008) 813.
- [29] J. Yang, J. Bei, S. Wang, *Biomaterials* 23 (2002) 2607.
- [30] Z.Q. Feng, X.H. Chu, N.P. Huang, M.K. Leach, G. Wang, Y.C. Wang, Y.T. Ding, Z.Z. Gu, *Biomaterials* 31 (2010) 3604.
- [31] L. He, C. Mu, J. Shi, Q. Zhang, B. Shi, W. Lin, *Int. J. Biol. Macromol.* 48 (2011) 354.
- [32] W. Xue, B.V. Krishna, A. Bandyopadhyay, S. Bose, *Acta Biomater.* 3 (2007) 1007.
- [33] E. Seyedjafari, M. Soleimani, N. Ghaemi, M.N. Sarbolouki, *J. Mater. Sci. Mater. Med.* 22 (2011) 165.
- [34] R.M. Salaszyk, W.A. Williams, A. Boskey, A. Batorsky, G.E. Plopper, *J. Biomed. Biotechnol.* 1 (2004) 24.
- [35] V. Karageorgiou, D. Kaplan, *Biomaterials* 26 (2005) 5474.
- [36] G. Ciardelli, P. Gentile, V. Chiono, M. Mattioli-Belmonte, G. Vozzi, N. Barbani, P. Giusti, *J. Biomed. Mater. Res. A* 92 (2010) 137.
- [37] H. Shen, X. Hu, F. Yang, J. Bei, S. Wang, *Biomaterials* 30 (2009) 3150.
- [38] C.D. Friedman, D. Costantino, S. Takagi, L.C. Chow, *J. Biomed. Mater. Res. B* 43 (1998) 428.